

## **Supplementary Materials**

*for*

Magnetic Carbon Foam adorned with Co/Fe  
Nanon-needles as an Efficient Activator of  
Oxone for Oxidative Environmental  
Remediation: Roles of Surficial and Chemical  
Enhancement

## **Text S1: Experimental details**

### **1.1 Chemicals and Reagents**

Chemical reagents involved in this study were commercially purchased and employed as received without further purifications. Cobalt nitrate hexahydrate ( $\text{Co}(\text{NO}_3)_2 \cdot 6\text{H}_2\text{O}$ ) (>98%) and  $\text{Fe}(\text{NO}_3)_3$  were obtained from Showa Chemicals (Japan). Tannic acid (99%) was purchased from Acros Organics (Belgium). Bis(4-hydroxyphenyl)methanone (BHPM), peroxymonosulfate (Oxone), methanol (MeOH) (99.9%), ethanol (>99.8%), *tert*-butanol (>99.5%), sodium azide ( $\text{NaN}_3$ ) (99.5%) were received from Sigma-Aldrich (USA). Deionized (D.I) water was prepared up to less than 18 M $\Omega$ -cm.

### **1.2 Catalytic activation of Oxone for BHPM degradation**

The catalytic degradation of BHPM by MCF activated Oxone was conducted using batch experiments. Typically, a small amount of MCF (i.e., 100 mg/L) was firstly added into a BHPM solution with the initial BHPM concentration ( $C_0$ ) of 5 mg/L for 15 min to verify whether BHPM might be adsorbed on MCF surface. Next, 150 mg/L of Oxone was quickly introduced into BHPM solution to initiate the degradation experiment. At a fixed reaction time ( $t$ ), sample aliquots were withdrawn from the BHPM solution, which were then filtrated by filters to separate MCF from the solution. The remaining BHPM concentration of the filtrate at  $t$  (min) ( $C_t$ ) was subsequently measured using high-performance liquid chromatography (HPLC) with a UV-vis detector (KNAUER Azura HPLC, Germany). A mixture of acetonitrile and water at a ratio of 1:1 was used as the mobile phase with a flow rate of 1.0 ml/min. The detection was carried out at 280 nm.

For experiments, the effects of different MCF dosages, Oxone dosages, BHPM initial concentrations, temperatures, initial pH values, co-existing substances and inhibitors were investigated. To explore the reactive radical species contributed to the degradation of BHPM by MCF+Oxone, electron paramagnetic resonance (EPR) was particularly employed using 5,5-Dimethyl-1-pyrroline N-oxide (DMPO) as a radical spin-trapping agent. The reusability of MCF for continuous Oxone activation to degrade BHPM was further performed by re-using MCF to multiple BHPM degradation cycles. For the recycle experiments, the used MCF was collected via centrifugation, washed thoroughly by D.I water several times before drying in an electric oven at 65 °C for 24 h, which is then employed for the subsequent degradation experiments. The intermediate products generated from BHPM degradation were also determined by a mass spectrometer (Thermo Finnigan Corporation, LCQ ion-trap mass spectrometer, USA).

Moreover, as ROS might be generated during the activation and involved in BHPM degradation, these species were necessarily determined by electron paramagnetic resonance (EPR) using 5,5-Dimethyl-1-pyrroline N-oxide (DMPO) and 2,2,6,6-tetramethylpiperidine (TEMP) as radical spin-trapping agents to reveal the mechanism of BHPM degradation. Besides, the intermediates derived from BHPM degradation were also determined using a mass spectrometer (Thermo Finnigan Corporation, mass spectrometer, USA). The Oxone concentration was monitored during the experiments of BHPM degradation at 30 °C. Sample aliquots were withdrawn, filtered through a 0.22- $\mu\text{m}$  PVDF filter, and injected to a mixture of 3 mL of KI solution (100 g/L KI containing 500 mg/L  $\text{NaHCO}_3$ ) and 2.5 mL DI water. The resulting solution was then measured with a UV-vis spectrophotometer (Chrom Tech

CT-2200, Taiwan) at 395 nm to determine Oxone concentrations. Degradation products of BHPM were then identified by liquid chromatography-mass spectrometry-mass spectrometry (Thermo TSQ Quantum, USA).

### 1.3 DFT calculation

The active sites on the BHPM molecule were visualized by HOMO, LUMO, electrostatic potential (ESP), and Fukui function using DFT calculation performed with the DMol<sup>3</sup> module. The exchange correlation functional of generalized gradient approximation (GGA) and the correction method of Perdew Burke Ernzerhof (PBE) were applied with spin unrestricted. During the calculation, the following parameters with the DNP basis set (basis file = 3.5) were used. Definition of Fukui function and Fukui indexes ( $f^-, f^0, f^+$ )

$$\text{Fukui function: } f(\mathbf{r}) = \left[ \frac{\partial \rho(\mathbf{r})}{\partial N} \right]_{\nu}$$

Where;  $\rho(\mathbf{r})$  is the electron density at a point  $\mathbf{r}$  in space;  $N$  is the electron number in the system;  $\nu$  is the external potential.

Fukui function ( $f$ ) in reaction:

$$\text{Nucleophilic attack: } f^+(\mathbf{r}) = \rho_{N+1}(\mathbf{r}) - \rho_N(\mathbf{r}) \approx \rho^{\text{LUMO}}(\mathbf{r})$$

$$\text{Electrophilic attack: } f^-(\mathbf{r}) = \rho_N(\mathbf{r}) - \rho_{N-1}(\mathbf{r}) \approx \rho^{\text{HOMO}}(\mathbf{r})$$

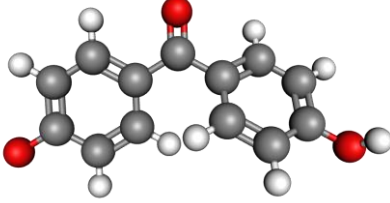
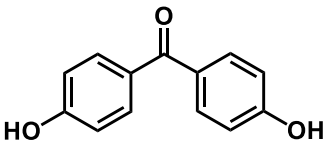
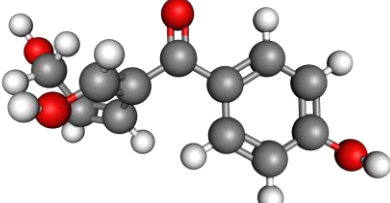
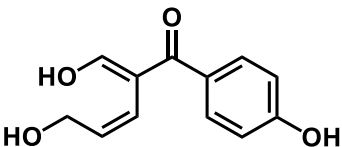
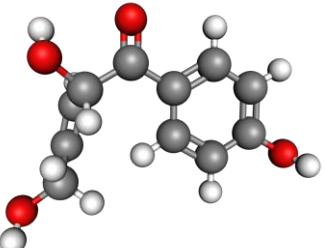
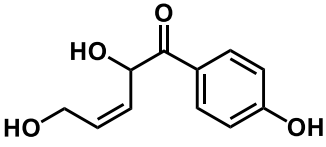
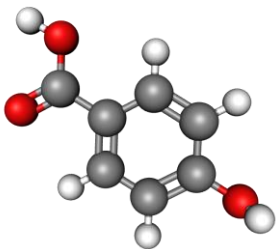
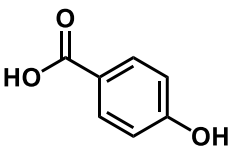
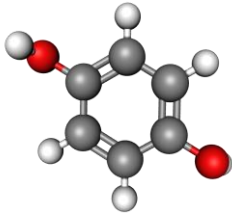
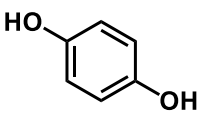
Radical attack:

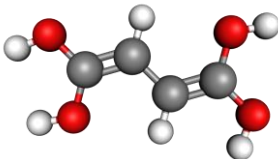
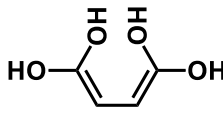
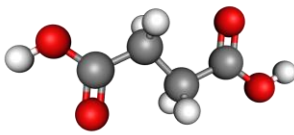
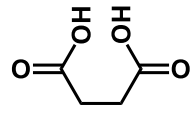
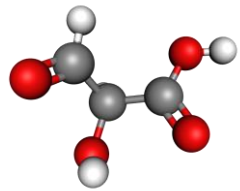
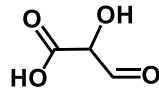
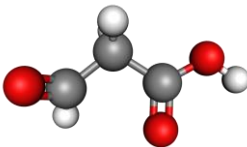
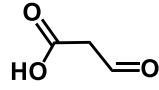
$$f^0(\mathbf{r}) = \frac{f^+(\mathbf{r}) + f^-(\mathbf{r})}{2} = \frac{\rho_{N+1}(\mathbf{r}) - \rho_{N-1}(\mathbf{r})}{2} \approx \frac{\rho^{\text{HOMO}}(\mathbf{r}) + \rho^{\text{LUMO}}(\mathbf{r})}{2}$$

Table S1. A comparison of activation energy ( $E_a$ ) between MCF+Oxone and other processes for degradation of UV stabilizers.

Catalyst	$E_a$ (kJ/mol)	Reference
MCF + Oxone	18.6	This work
CFNB + Oxone	54.4	(Cong Khiem, Dinh Tuan et al. 2022)
CFNS + Oxone	33.3	(Cong Khiem, Dinh Tuan et al. 2022)
CFNP + Oxone	43.6	(Cong Khiem, Dinh Tuan et al. 2022)
CoS + Oxone	42.7	(Liu, Yang et al. 2022)

Table S2. Detected by-products of BHPM degradation by MCF+Oxone

Label	3D Structure	Molecular structure
BHPM		 <b>Chemical Formula:</b> C <sub>13</sub> H <sub>10</sub> O <sub>3</sub> <b>m/z:</b> 214
M1.		 <b>Chemical Formula:</b> C <sub>12</sub> H <sub>12</sub> O <sub>4</sub> <b>m/z:</b> 220
M2.		 <b>Chemical Formula:</b> C <sub>11</sub> H <sub>12</sub> O <sub>4</sub> <b>m/z:</b> 208
M3.		 <b>Chemical Formula:</b> C <sub>7</sub> H <sub>6</sub> O <sub>3</sub> <b>m/z:</b> 138
M4.		 <b>Chemical Formula:</b> C <sub>6</sub> H <sub>6</sub> O <sub>2</sub> <b>m/z:</b> 110

M5.		 <b>Chemical Formula:</b> C <sub>4</sub> H <sub>6</sub> O <sub>4</sub> <b>m/z:</b> 118
M6.		 <b>Chemical Formula:</b> C <sub>4</sub> H <sub>6</sub> O <sub>4</sub> <b>m/z:</b> 118
M7.		 <b>Chemical Formula:</b> C <sub>3</sub> H <sub>4</sub> O <sub>4</sub> <b>m/z:</b> 104
M8.		 <b>Chemical Formula:</b> C <sub>3</sub> H <sub>4</sub> O <sub>3</sub> <b>m/z:</b> 88

**Table S3. Toxicity classification according to the Globally Harmonized System of Classification and Labelling of Chemicals<sup>§</sup>**

<b>Toxicity range (mg/L)</b>	<b>Classification</b>
<b>LC<sub>50</sub> ≤ 1</b>	Very toxic
<b>1 &lt; LC<sub>50</sub> ≤ 10</b>	Toxic
<b>10 &lt; LC<sub>50</sub> ≤ 100</b>	Harmful
<b>LC<sub>50</sub> &gt; 100</b>	Not harmful

<sup>§</sup> LC<sub>50</sub>, Half lethal concentration

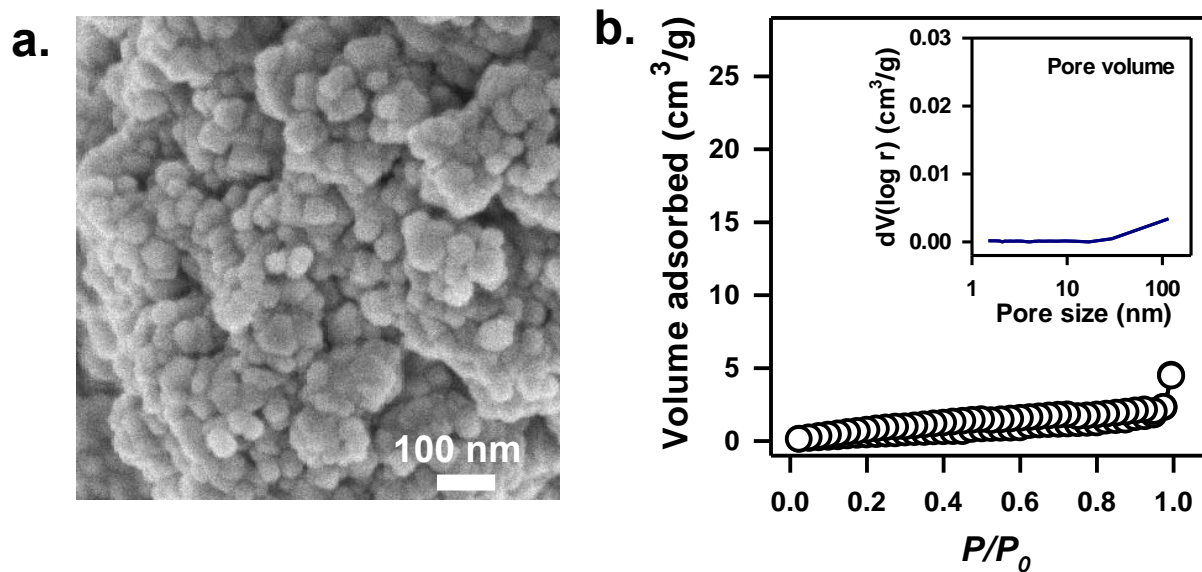


Figure S1. (a) SEM image and (b) textural properties of industrially available  $\text{Co}_3\text{O}_4$  (purchased from Alfa Aesar).

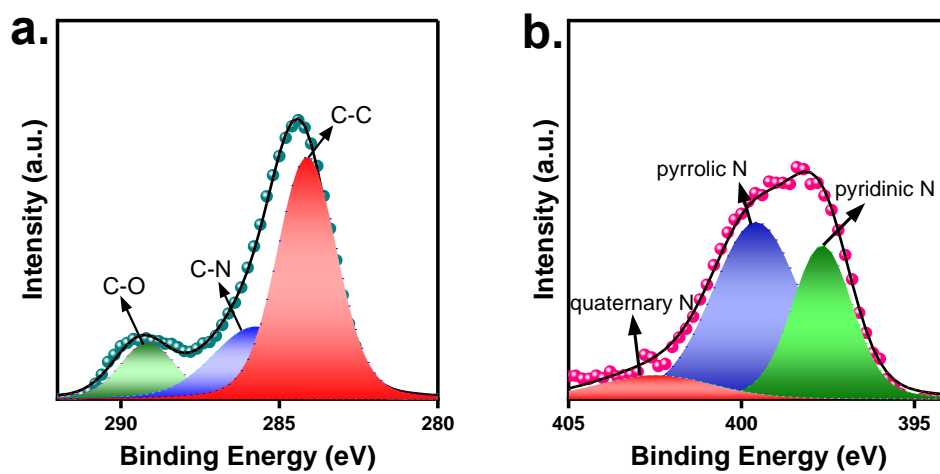


Figure S2. XPS spectroscopy of CF: (a) C1s (b) N1s.

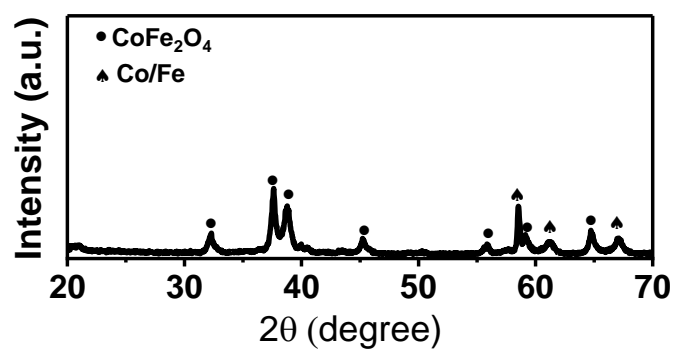


Figure S3. The XRD pattern of used MCF.

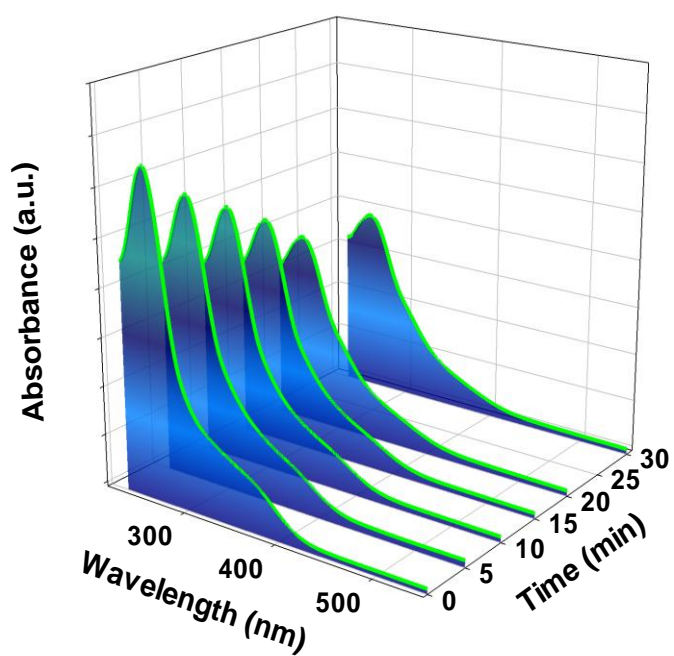
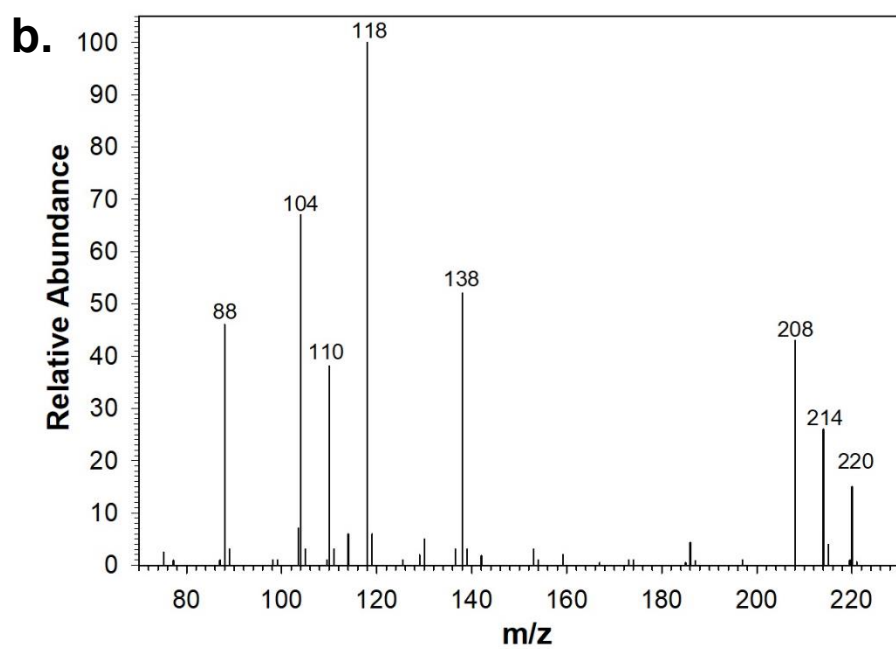
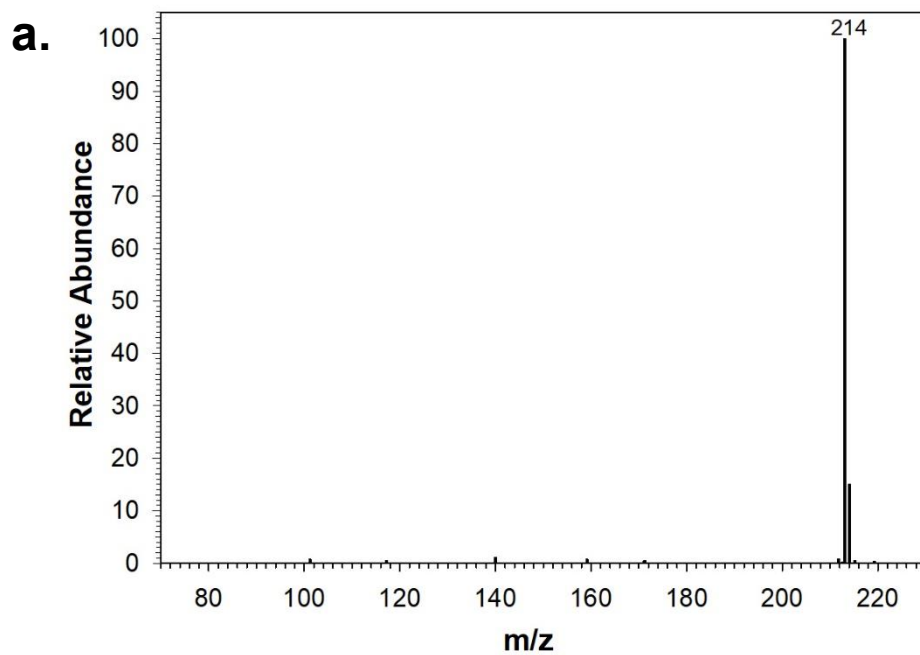


Figure S4. (a) Determination of superoxide by the NBT test



**Figure S5.** ESI mass spectra of (a) BHPM and (b) intermediates of BHPM degradation.